Steel and Composite Structures, Vol. 10, No. 6 (2010) 517-539
DOI: http://dx.doi.org/10.12989/scs.2010.10.6.517

Axial compressive behaviour of stub concrete-filled columns with elliptical stainless steel hollow sections

X. Dai and D. Lam*

School of Engineering Design and Technology, University of Bradford, UK

(Received June 22, 2010, Accepted November 2, 2010)

Abstract. This paper presents the axial compressive behaviour of stub concrete-filled columns with elliptical stainless steel and carbon steel hollow sections. The finite element method developed via ABAQUS/ Standard solver was used to carry out the simulations. The accuracy of the FE modelling and the proposed confined concrete stress-strain model were verified against experimental results. A parametric study on stub concrete-filled columns with various elliptical hollow sections made with stainless steel and carbon steel was conducted. The comparisons and analyses presented in this paper outline the effect of hollow sectional configurations to the axial compressive behaviour of elliptical concrete-filled steel tubular columns, especially the merits of using stainless steel hollow sections is highlighted.

Keywords: concrete-filled column; elliptical hollow section; stainless steel; nonlinear finite element model; axial compressive behaviour; parametric study.

1. Introduction

Concrete-filled steel tubular composite columns comprise a combination of steel and concrete and utilise the most favourable properties of both constituent materials. The interaction between the steel hollow section and concrete core makes the composite column perform better structurally than individual constituent members but without significant increases in cost. Concrete-filled steel tubular columns are being used increasingly in modern buildings attributing to their excellent axial load carrying capacity and ductility. The practice of concrete-filled steel tubular columns in constructions can be traced back to 40 years ago. Extensive researches were carried out worldwide to investigate the structural behaviour of composite columns, which included the effects of geometrical features (Schneider 1998, Giakoumelis and Lam 2004, O'Shea and Bridge 1997,2000, Sakino *et al* 1998), concrete compaction (Han and Yang 2001, Han and Yao 2004) and high strength concrete (Uy 1998a, Gibbons and Scott 1996, Rangan and Joyce 1992) to the compressive load bearing capacity, the strength and buckling behaviours of concrete-filled steel tubular columns with square and rectangular hollow sections (Uy 1998b, 2001a, 2001b, Han and Yao 2003, Mursi and Uy 2003, Lam and Williams 2004, Han 2002). Although the outcomes from previous researches gave design guidance for concrete-filled composite columns, little literature can be found on composite columns with steel elliptical hollow sections and in particularly; stainless steel elliptical hollow sections. Following the increases in use of the concrete-

* Corresponding author, Professor, E-mail: d.lam1@bradford.ac.uk

filled steel tubular columns in model constructions, hollow sections made from stainless steel have attracted a significant attention from engineers and architects owing to their aesthetic appearance and structural efficiency.

Unlike carbon steel, stainless steel possesses natural corrosion resistance and bright surface; its surface may be exposed without any protective coating. Although the use of stainless steel for structural elements has the high initial material cost, but when it is considered on a whole-life basis, cost comparisons with other metallic materials become more favourable (Gardner *et al* 2007). Unlike composite columns with carbon steel hollow sections, concrete filled columns with stainless steel hollow sections maintain their durable and aesthetic exposed surfaces; in addition to the higher strength and ductility associated with the stainless steel sections which may lead to higher load bearing capacity and better ductility or reduction in column sizes, both of which have clear economic incentives. The structural behaviour of stainless steel tubular members has been studied worldwide (Young and Lui 2005, Ellobody and Young 2005, Gardner *et al* 2006). These investigations have led to an expansion of the scope of Eurocode 3: Part 1.4 (CEN 2006) to now cover cold-formed stainless steel grades. Although recent researches into buckling and compressive behaviour of stainless and carbon steel elliptical hollow sections were broadly carried out (Gardner and Chan 2007, Chan and Gardner 2008a, 2008b, 2009, Ruiz-Teran and Gardner 2008, Theofanous *et al* 2009a, 2009b), researches into the structural behaviour and design rules of concrete-filled composite columns with stainless steel hollow sections were rather limited although some studies were reported by Young and Ellobody (2006), Ellobody and Young (2006), Lam and Gardner (2008) and Dabaon *et al* (2009).

The main objective of the research presented in this paper is to investigate the axial compressive behaviour of stub concrete-filled composite columns with elliptical hollow sections with stainless steel and carbon steel hollow sections. The aim includes three folds: (1) to extend a nonlinear finite element numerical modelling method proposed by Dai and Lam (2010) to cover elliptical hollow sections with stainless steel hollow sections; (2) to compare the axial compressive behaviour of stub concrete-filled composite columns with typical carbon steel and stainless steel elliptical hollow sections; (3) to provide useful information to structural steel manufacturers and building industries.

2. Experimental study

2.1 Specimens and test arrangement

A series of stub concrete-filled composite columns with stainless steel and carbon steel elliptical hollow sections were tested to investigate the axial compressive behaviour and failure modes. For each test, horizontal and vertical strain gauges were attached to the steel surface at middle height, as shown in Fig. 1(a), to measure the hoop and axial strains respectively. Linear variable displacement transducers (LVDT) were placed between the loading and bearing plates of the specimen to record the full axial shortening. The testing set-up is shown in Fig. 1(b) (c).

The dimensions of test specimens and their material properties are given in Table 1, which included the column length, section configurations and materials properties: stainless steel (specimens SS1~SS6) and carbon steel (specimens CS1~CS9). Three concrete grades, C30, C60 and C100, representing normal to high strength concrete, were used for concrete infill.

Coupons were cut from the elliptical hollow sections and tested to EN10002-1 (2001) to determine the tensile strength. The coupons were cut from the region of maximum radius of curvature (i.e., the

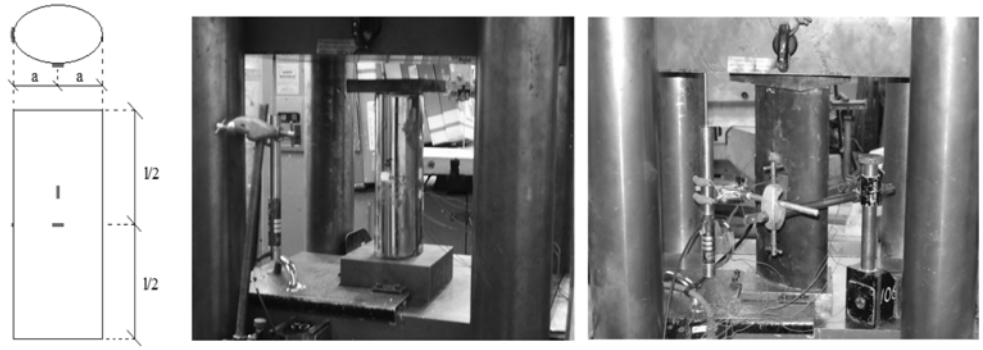

(a) Locations of strain gauges

(b) Test set-up of a column with elliptical stainless steel tube

(c) Test set-up of a column with elliptical carbon steel tube

Fig. 1 Test arrangement

Table 1 Summary of specimen dimensions and material references and comparison of maximum loads from experiments and numerical predictions

Tested specimen reference	Elliptical hollow section (EHS) dimensions, 2a × 2b × t (mm)	EHS length, L (mm)	Steel material reference	Infilled concrete grade reference	Maximum load by test, P_{Test}(kN)	Maximum load by FE model, P_{FE} (kN)	P_{Test}/ P_{FE}
SS1	123.0 × 77.0 × 1.88	243	SSteel-1	S-C30	551	517	1.066
SS2	124.1 × 76.4 × 1.88	244	SSteel-1	S-C100	857	858	0.999
SS3	121.0 × 78.4 × 2.98	242	SSteel-2	S-C30	680	688	0.988
SS4	121.3 × 78.0 × 3.00	242	SSteel-2	S-C100	1065	1003	1.061
SS5	85.5 × 57.0 × 3.17	176	SSteel-3	S-C30	492	493	0.998
SS6	85.4 × 57.3 × 3.20	174	SSteel-3	S-C100	570	530	1.075
CS1	150.40 × 75.60 × 4.18	300	CSteel-1	C-C30	839	821	1.021
CS2	150.57 × 75.52 × 4.19	300	CSteel-1	C-C60	974	952	1.023
CS3	150.39 × 75.67 × 4.18	300	CSteel-1	C-C100	1265	1170	1.081
CS4	150.12 × 75.65 × 5.12	300	CSteel-2	C-C30	981	951	1.031
CS5	150.23 × 75.74 × 5.08	300	CSteel-2	C-C60	1084	1078	1.006
CS6	150.28 × 75.67 × 5.09	300	CSteel-2	C-C100	1296	1303	0.995
CS7	148.78 × 75.45 × 6.32	300	CSteel-3	C-C30	1192	1134	1.051
CS8	148.92 × 75.56 × 6.43	300	CSteel-3	C-C60	1280	1238	1.034
CS9	149.53 × 75.35 × 6.25	300	CSteel-3	C-C100	1483	1434	1.034
						Mean	1.031
						COV	0.030

flattest portion of the section) and milled to specification. Some flattening of the ends occurred while gripping the specimen but this was well away from the 'neck' of the sample. The measured stress-strain curves are shown in Fig. 2 and the main parameters are summarized in Table 2. The material references for the three wall thicknesses of 2 mm, 3 mm and 3.2 mm are given as "SSteel-1", "SSteel-2" and "SSteel-3" respectively. The carbon steel material references for the three section wall thicknesses of

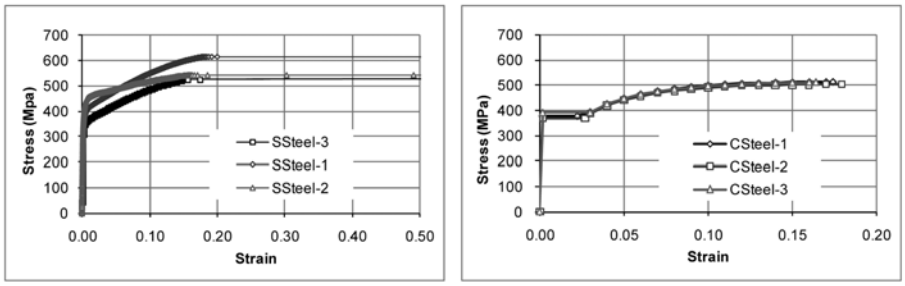

(a) Stainless steel coupon test (b) Carbon steel coupon test

Fig. 2 Measured stress-strain relationships of steel materials

Table 2 Main parameters for the material properties of steel tubes from coupon tests

Material type	Steel tube material reference	Section thickness, t (mm)	Elastic modulus, E (MPa)	Yield strength, f_y (MPa)	Ultimate strength, f_u (MPa)
Stainless steel	SSteel-1	2.0	193,300	377.0	615
	SSteel-2	3.0	194,100	420.0	544
	SSteel-3	3.2	194,500	339.0	526
Carbon steel	CSteel-1	4.0	217,500	376.5	513
	CSteel-2	5.0	217,100	369.0	505
	CSteel-3	6.3	216,500	400.5	512

4 mm, 5 mm and 6.3 mm are defined as “CSteel-1”, “CSteel-2” and “CSteel-3”. From the steel coupon tests, the following points can be observed: (1) the elastic modulus of stainless steel was slightly lower than that of carbon steel; (2) after the proportional limit, there is no yield plateau for the stainless steel material; (3) the average yield strength of the stainless steel was a little lower than that of carbon steel (378.7 Mpa for stainless steel and 381.7Mpa for carbon steel respectively), however, the average ultimate strength of stainless steel is evidently higher than that of the carbon steel (561.7 Mpa and 510 Mpa respectively); (4) stainless steel material possesses better ductility. Concrete cubes and cylinders, casted using the same batch concrete for each column specimen were tested to determine the concrete properties. The measured unconfined concrete cube and cylinder compressive strengths on test day are given in Table 3.

2.2 Summary of experimental observations

Fig. 3 presents the axial compressive load to end-shortening characteristics and Table 1 listed the

Table 3 Measured compressive strengths of the concrete infill (Test day)

Infilled concrete grade reference	Unconfined compressive cubic strength, $f_{ck,\,cub}$(MPa)	Unconfined compressive cylinder strength, f_{ck} (MPa)
S-C30	47	37
S-C100	109	89
C-C30	36.9	30.5
C-C60	59.8	55.3
C-C100	102.2	98.4

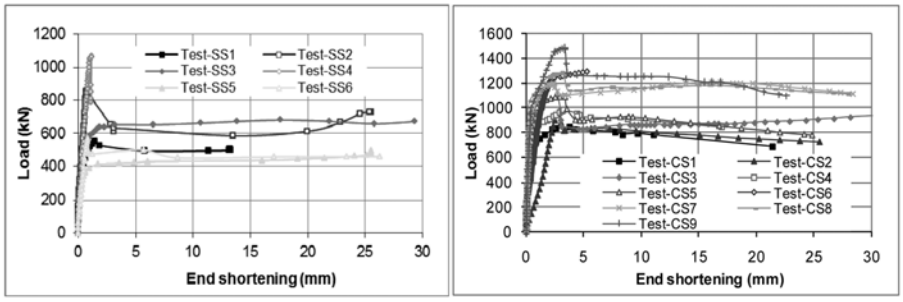

(b) CFT columns with stainless steel tubes (a) CFT columns with carbon steel tubes

Fig. 3 Measured load-end shortening curves

maximum recorded axial loads for the fifteen stub concrete-filled tubular columns with elliptical steel hollow sections. Base on the experimental observation, the following conclusions may be drawn: (1) increases in the concrete infill's strength, leads to increases in the maximum axial compressive loads, however, the residual load capacity of a column with high strength concrete was only slightly higher than that of a column filled with normal concrete. This indicates once the concrete core cracked or crushed, the unconfined concrete strengths no longer dominates the axial load bearing capacity of the concrete filled column; (2) the compressive capacity and the ductility of a stub column with a thicker section wall was evidently higher than that of the column with a thinner wall thickness. This indicates that increases in the steel thickness thus leads to increases in load bearing capacity and ductility. Moreover, the thicker wall thickness also improved the confinement effect to the concrete core and thus improved the overall compressive capacity of the composite columns; (3) for stub columns filled with high strength concrete, there was an evident "drop" in the load vs. end-shortening curve, however, this is not evident for columns filled with normal strength concrete; (4) generally, the load vs. end-shortening curves for concrete-filled stub columns with stainless steel hollow sections and with carbon steel sections are very similar except that specimens with stainless steel sections had shown better ductility in test.

As shown in Fig. 1, the stub column was placed between a loading plate and a bearing plate. During the loading process the loading plate was pushed down gradually to apply the compressive force to the column. Observation during the tests showed, for most tested specimens, that the deformation (bulge) initiated from the column ends, then with the stress and strain redistribution over the whole specimen, larger deformation and buckling appeared at the middle of the hollow section. Fig. 4 shows the final deformation (failure modes) of some typical tested stub columns, evident bulges occurred at the middle height and both ends of the steel tubes. In addition, visible shear failure in the concrete core was observed in some columns with thinner wall thickness (SS1, CS1 and CS4). There was no significant difference in the failure modes of carbon steel hollow sections and stainless steel hollow sections.

3. Finite element modelling

3.1 General

Experimental studies provide a very effective and reliable method in understanding the behaviour of

Fig. 4 typical failure modes

the structural members, however it is an un-denied fact that the experimental studies are expensive, time consuming. Numerical finite element models may be developed through commercial software packages to predict the behaviour of structural members. For stub concrete-filled steel tubular columns in compressions, the structural behaviour and failure modes were characterized by yielding of the hollow sections and concrete crushing, which differed from slender concrete-filled steel tubular columns under axial compressions whose failure mode generally being global buckling, this hinted that in the simulation of stub concrete-filled composite columns, the confinement effect must be considered.

3.2 Summary of typical finite element (FE) model features

The nonlinear finite element model developed through ABAQUS/Standard solver used to model elliptical concrete-filled steel stub columns under axial compression, as shown in Fig. 5, has been successfully used in predicting the compressive behaviour of stub concrete-filled elliptical steel columns (Dai and Lam 2010). In which three-dimensional solid elements (C3D8) were used to model the main column components: elliptical steel hollow section and confined concrete core. Two rigid plates were used to model the loading and bearing plates at both ends of the stub composite column. The followings summarized the selection of some of the main modelling parameters

(1) Based on the sensitivity study of the mesh sizes, the appropriate element size should be 5~10 mm for the steel hollow section and 10~20 mm for the concrete core, *i.e.,* the concrete element sizes should be about two times the element sizes of the steel hollow section.

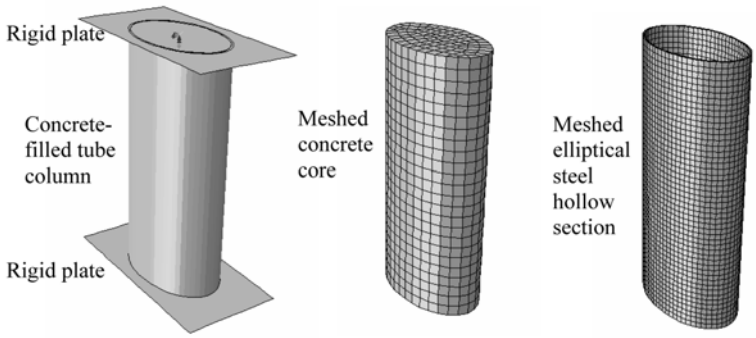

Fig. 5 Typical FE model adopted in numerical modelling

(2) All contacts between constituent members (including steel tube to concrete core, end plate to column end section) were defined as surface-to-surface contacts with a finite sliding option and any gap between the contacting surfaces were ignored before loading in the modelling. However during loading, the contact pair may keep contacted or open to form a gap. "Hard contact" in ABAQUS was used for the normal contact behaviour to avoid penetration but contact pair reopening was allowed after contacted. "Rough" friction was used in the tangential direction of the contact pairs to restrain the slip between the rigid plate and the column end. A friction coefficient of 0.2~0.3 was used for the tangential direction of the contact to consider the binding interaction between hollow section and concrete core after a series of comparisons and analyses.

(3) The concrete Poisson's ratio of 0.2 was selected for the concrete to model the axial compressive behaviour of stub concrete-filled composite columns with elliptical hollow sections.

(4) In the FE model, the lower rigid plate contacting to the bottom of the column was fixed in all six directions by the reference node and the upper rigid (loading) plate to the top of the column was fixed in five directions and only allowed movement in column axis at the reference node. The column end restraints adopted in the FE model were identical to the testing procedures; no other translations and rotations were observed in tests at both loading plates. The load was applied as static uniform displacement at the upper rigid plate through the reference node at the centre of rigid plate, which is also identical to the experimental loading procedure.

(5) It is inevitable that a steel tube may have imperfections, such as varied wall thickness, changeable cross section shape etc., however for the stub concrete filled steel tube column, the imperfection were very small. Due to the imperfection was not measured in test, therefore, in the numerical modelling, any imperfection was ignored. However it must be pointed out, any imperfection will certainly reduce the load capacity of the stub columns.

3.3 Stress-stain model of confined concrete

The compressive strength of confined concrete is different from that of unconfined concrete, which depends on the confinement conditions. Previous research (Giakoumelis and Lam 2004) on concrete-filled stub tubular columns revealed that circular steel tube with a lower value of diameter over wall thickness (D/t) ratio provided higher confinement to the concrete core owing to the restraining action and inverse for steel tube with higher D/t ratio. Due to the restraining action executed through the contact interaction between the concrete core surface and the inner surface of the steel hollow section, hollow section shape may affected the total confinement effect and the confining force distribution along the perimeter of the tube. Thus the stress-strain relationship of the confined concrete with different hollow sections might be different. The special stress-strain relationship for confined concrete filled in elliptical steel hollow sections proposed by Dai and Lam (2010) was validated for concrete confined in carbon steel hollow sections EHS 150 × 75 mm with wall thickness of 4 mm, 5 mm and 6.3 mm. This model will be modified in the research presented in this paper to extend the hollow section dimension range and covered the stub concrete filled columns with elliptical stainless steel hollow sections.

The basic form of the stress-strain relationship for the unconfined and confined concrete in elliptical steel hollow section is shown in Fig. 6, where f_{ck} is the unconfined compressive cylinder strength of concrete ($f_{ck} = 0.8f_{ck,cub}$ and $f_{ck,cub}$ is the unconfined compressive cube strength of concrete). The strain ε_{ck} corresponding to f_{ck} for unconfined concrete may be taken as 0.003 according to ACI 318-95 (1999).

The maximum strength f_{cc} and corresponding strain ε_{cc} of confined concrete are determined by Eq. (1)

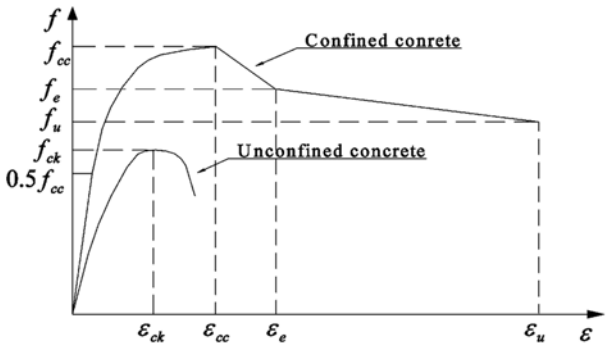

Fig. 6 Stress-strain curves of concrete unconfined and confined by elliptical hollow sections

$$f_{cc} = f_{ck} + k_1 f_l \tag{1a}$$

$$\varepsilon_{cc} = \varepsilon_{ck}\left(1 + k_2 \frac{f_l}{f_{ck}}\right) \tag{1b}$$

Considering the confinement effect of the hollow sections from a circular shape to an arbitrary elliptical shape, modified parameters for Eq. (1) are proposed. According to the research by Richart *et al* (1928), Yang *et al* (2008), Hu and Schnobrich (1989) and Hu *et al* (2003), the authors suggested that the following parameters in Eq. (2) for concrete-filled elliptical steel tube columns with elliptical steel hollow sections

$$k_1 = 6.770 - 2.645(a/b) \tag{2a}$$

$$k_2 = 20.5 \tag{2b}$$

$$f_l = f_y\left\{e^{-1.3\left(\frac{a+b}{t}\right)^{0.34}}\right\} \tag{2c}$$

where,

a = the long radius of the elliptical hollow steel section
b = the short radius of the elliptical hollow steel section
t = the wall thickness of the elliptical hollow section
f_y = the yield strength of the elliptical hollow steel section

The first part of the stress strain curve defines the linear property of the confined concrete and the proportional limit stress can be assumed to be $0.5f_{cc}$ (Hu *et al* 2003, Ellobody *et al* 2006). The initial Young's modulus of the confined concrete followed the empirical formulation provided in ACI 318-95 (1999) and expressed as $E'_{cc} = 4700\sqrt{f_{cc}}$ MPa. The Poisson ratio of the confined concrete may be taken as 0.2.

The second part of the stress-strain model specifies the nonlinear portion which starts from the

proportional limit stress $0.5f_{cc}$ and ends at the maximum confined concrete strength f_{cc}. This part was proposed by Saenz (1964) and described as Eq. (3), which has been validated by Ellobody *et al* (2006), and Dai and Lam (2010) in numerical modelling of circular concrete-filled steel tube stub columns and elliptical concrete-filled steel tube columns under axial compression.

$$f = \frac{E_{cc}\varepsilon}{1 + (R + R_E - 2)\left(\frac{\varepsilon}{\varepsilon_{cc}}\right) - (2R - 1)\left(\frac{\varepsilon}{\varepsilon_{cc}}\right)^2 + R\left(\frac{\varepsilon}{\varepsilon_{cc}}\right)^3} \tag{3}$$

where, $R_E = \frac{E_{cc}\varepsilon_{cc}}{f'_{cc}}, R = \frac{R_E(R_\sigma - 1)}{(R_\varepsilon - 1)^2} - \frac{1}{R_\varepsilon}, \quad R_\sigma = R_\varepsilon = 4.$

The third part of the stress-strain curve begins from the maximum confined concrete strength f_{cc} and terminates at:

$$f_e = \left(\frac{b}{a}\right)^2\left(\frac{\varepsilon_u - \varepsilon_e}{\varepsilon_u - \varepsilon_{cc}}\right)(f_{cc} - f_u) + f_u \tag{4}$$

For $15 \le (a + b)/t \le 65$ and $1 \le a/b \le 2$. The corresponding strain is taken to be $\varepsilon_e = 10\varepsilon_{ck}$.

The fourth part of the curve starts from f_e and terminates when $f_u = k_3 f_{cc}$ with the corresponding strain $\varepsilon_u = 30\varepsilon_{ck}$. At this stage, local buckling of the stainless steel tube might have occurred; the value of parameter k_3 will depend on the strength of concrete. $k_3 = 0.7$ for C30 concrete and 0.35 for C100 concrete. Linear interpolation may be used for concrete between C30 and C100 based on the realistic concrete strength, but f_u is suggested not less than 30 MPa.

4. Validation of finite element model

Using the FE numerical method and proposed stress-strain model for confined concrete described in the aforementioned sections, fifteen tested specimens were modelled to verify the accuracy of the numerical method. In these simulations, the compressive stress-strain constitutive relationships of confined concrete were deduced from the measured unconfined concrete compressive strength according to the proposed confined concrete stress-strain model. The material properties of the steel hollow sections were based on the material testing as described in the experiment sections.

4.1 Comparison of load vs. end shortening characteristics

A comparison of maximum axial compressive loads between numerical predictions (P_{FE}) and experimental results (P_{Test}) are presented in Table 1 and Fig. 7 showing typical load vs. end shortening curves, it can be seen very good agreements were achieved. The comparisons indicate that the finite element model developed through ABAQUS/Standard solver, combining with the special compressive stress-strain model proposed for confined concrete in elliptical steel hollow sections successfully predicted the main axial compressive behaviour of stub concrete filled composite columns with elliptical stainless steel and carbon steel hollow sections. In particular, the numerical model was able to capture the post failure behaviour after the stub columns experienced the peak load.

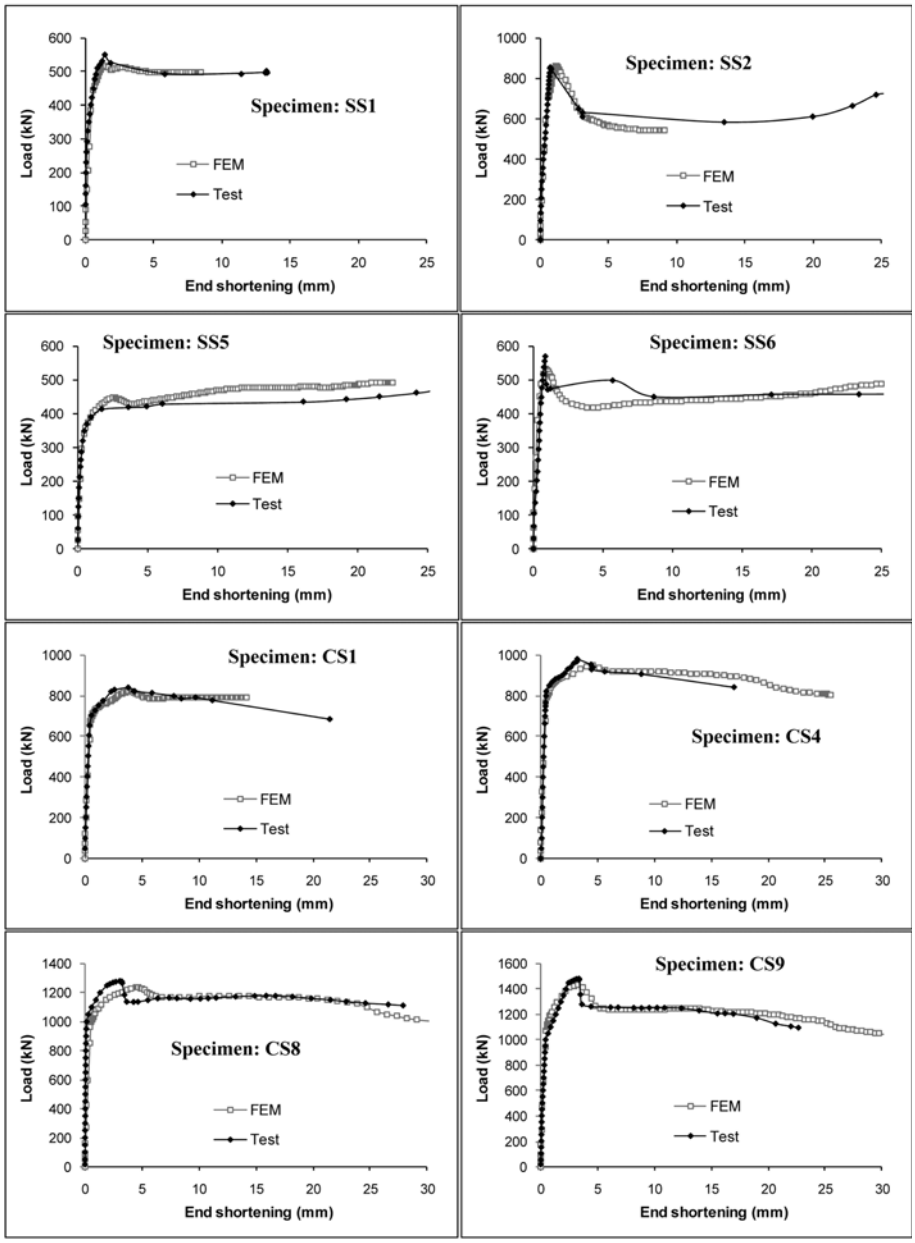

Fig. 7 Comparison of typical axial load to end-shortening curves by numerical prediction and experimental observation

4.2 Comparison of the failure modes

A comparison of failure modes of typical concrete-filled steel tube columns predicted by numerical models and observed from experiments is shown in Fig. 8. The finite element models revealed some important failure patterns, such as outwards buckling, bulges near the ends and the middle section of the columns.

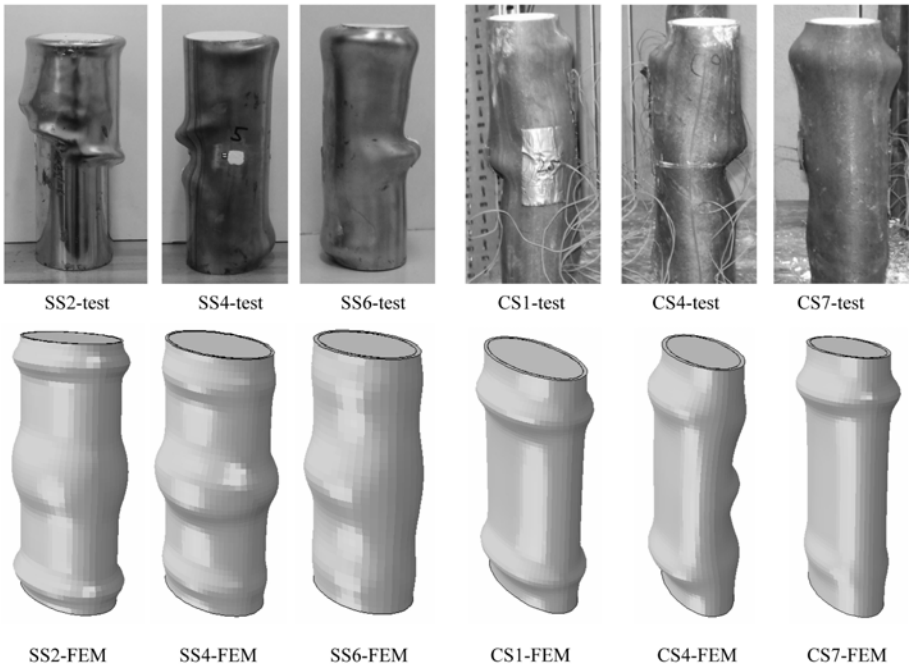

Fig. 8 Comparison of failure modes observed from experiments and predicted by FEMs

5. Comparison and analysis of axial compressive behaviour of concrete filled elliptical hollow sections

There are many factors that might be used to characterize the axial compressive behaviour of concrete filled columns with elliptical steel hollow sections. For example, the maximum load vs. end-shortening may be used to reflect the load bearing capacity and ductility of the composite columns. This section will compare the axial compressive behaviour of concrete-filled columns with elliptical steel hollow sections and discuss the effect of geometrical and material properties to the structural behaviour. Besides the maximum axial compressive load and end-shortening, two indices namely strength enhancement index, *SI* and ductility index, *DI* are introduced to describe the axial compressive behaviour. Three other factors describing the column sectional characteristics: section constraining factor, ξ, section strength factor, γ and section aspect ratio, α were introduced to explore the effect of the section properties to the structural behaviour. The effect of the material properties of steel hollow sections and infill concrete strength to the axial compressive behaviour will also be highlighted throughout the parametric study.

5.1 Definition of parameters

5.1.1 Strength enhancement index, SI

The strength enhancement index, *SI* describes in this paper is defined as the ratio of the maximum compressive load of the concrete-filled tube column to the sum of the strengths of the individual constituent components (concrete core and steel hollow section tube). This parameter reflects the

contribution of steel-concrete composite action. *SI* value higher than 1.0 represents the positive interaction between the steel hollow section and the concrete core resulted from concrete confinement effect which delay or elimination the local buckling in the hollow section. The formula for the strength enhancement index, *SI* is given in Eq. (5) below

$$SI = \frac{N_m}{A_s f_y + A_c f_{ck}} \tag{5}$$

where N_m is the maximum compressive load of concrete-filled stub column; A_s and f_y are the cross-sectional area and material yield strength of the hollow section; A_c and f_{ck} are the cross-sectional area and unconfined compressive cylinder strength of concrete core.

5.1.2 Ductility index DI

The ductility index, *DI* is defined as the inverse ratio of the axial end-shortening of the concrete-filled stub column, δ_m, corresponding to the maximum load N_m to the axial end-shortening of the stub column, $\delta_{85\%m}$, corresponding to the compressive load being 85% of the maximum load N_m after the column experienced the maximum load. Higher *DI* value represents that the concrete-filled columns have better ductility. The ductility index, *DI* is expressed in Eq. (6)

$$DI = \frac{\delta_{85\%m}}{\delta_m} \tag{6}$$

5.1.3 Section constraining factor ξ

The section constraining factor, ξ is defined as the ratio of the yield strength of steel hollow section to the compressive strength of the concrete core section. The higher value of ξ indicates the steel tube may provide stronger confinement to the concrete core although the actual confinement effect may be affected by other factors, such as the section strength factor, γ and section aspect ratio, α etc. The formula for the section constraining factor, ξ is given in Eq. (7)

$$\xi = \frac{A_s f_y}{A_c f_{ck}} \tag{7}$$

where A_s, f_y, A_c and f_{ck} are specified as those in Eq. (5).

5.1.4 Section strength factor γ

The section strength factor, γ is similar to the ratio of the diameter to wall thickness for a circular hollow section. It is specified as the ratio of the average of the two outer diameters to the wall thickness. The steel tube with a higher γ value suggests weaker section constraining strength and less confinement to the concrete core due to either thinner section wall thickness or larger section diameters. For elliptical hollow section, the expression, γ is given in Eq. (8)

$$\gamma = \frac{a + b}{t} \tag{8}$$

where, a and b are the long and short outer radii of the elliptical hollow section and t is the wall thickness.

5.1.5 Section aspect ratio α

The section aspect ratio α is defined as the ratio of the long outer radius to the short outer radius of the elliptical section, which is described in Eq. (9) below

$$\alpha = \frac{a}{b} \tag{9}$$

where a, b are termed as those given in Eq. (8). This parameter reflects an important feature of the hollow section geometrical shape. For a circular section, $\alpha = 1$, for an elliptical section, $\alpha > 1$. The section aspect ratio may affect the concrete confinement effect, and bending and buckling characteristics of the tubular columns.

5.2 Parametric study

45 concrete-filled stub columns with different elliptical section configurations (including 9 circular hollow sections) from 160 × 100 mm to 300 × 300 mm with wall thickness from 3 mm to 8 mm and three concrete grades, C30, C60 and C100 as shown in Table 4, were selected for the parametric study. To compare the effect of steel material properties to the axial compressive behaviour of composite columns, two typical stress-strain curves for stainless steel and carbon steel hollow section were adopted, therefore in total, 90 numerical simulations were performed.

Fig. 9 shows the stress-strain relationships of a typical stainless steel and carbon steel materials employed for the parametric study. Both were adjusted to have identical proportional limit of 323 MPa, identical initial elastic modulus of 200 GPa and identical yield strength or 0.2% proof strength of 350 MPa, but the maximum strength and corresponding strain were different. The ultimate strength and corresponding strain for stainless steel were 746 MPa and 0.363, and 514 MPa and 0.173 for the carbon steel. The failure strength and strain were 670 MPa and 0.413 for the stainless steel and 448 MPa and 0.24 for the carbon steel. In the current composite columns design codes, only the yield strength of material was taken into consideration and the effect of ultimate strength and ductility were ignored, this will certainly underestimate the potential of a composite tubular columns form with high strength and high ductility materials. By using these selected material models to investigate the axial compressive behaviour of concrete-filled composite columns, the effects of material yield strength, ultimate strength and ductility of the stainless steel to the compressive behaviour can be explored.

In the parametric study, the unconfined compressive cylinder strength of the infill concrete grade C30 and C100, represent normal strength concrete and high strength concrete, were based on experimental data (as shown in Table 3) The compressive cylinder strength of concrete grade C60 were assumed to be 64 MPa due to no experimental data is available. The compressive cylinder strengths for the unconfined concrete used in the parametric study are summarized in Table 5.

5.3 Discussion

The compressive behaviour of the 45 stub composite columns with stainless steel hollow sections was compared with that of the 45 identical composite columns with carbon steel hollow sections. Fig. 10 shows an example of axial compressive load vs. end shortening curves for 4 typical composite columns with different materials and concrete grades. It indicates that the composite columns with stainless steel hollow sections not only have higher axial load bearing capacity but also better ductility when

Table 4 Summary of dimensions and main parameters for selected concrete-filled tubular columns and comparison of compressive behaviour by numerical predictions

Model case ref.	EHS dimension 2ax2bxt (mm)	Infilled concrete grade	γ	α	Carbon steel EHS				Stainless steel EHS			
					ξ	N_{max} (kN)	SI	DI	ξ	N_{max} (kN)	SI	DI
C1	160 × 100 × 3	C30	43	1.6	0.90	909	1.12	>5.00	0.80	936	1.22	>5.00
C2	160 × 100 × 4.5	C30	29	1.6	1.41	1317	1.35	>5.00	1.25	1377	1.51	>5.00
C3	160 × 100 × 6	C30	22	1.6	1.96	1685	1.48	>5.00	1.73	1799	1.71	>5.00
C4	200 × 120 × 3	C30	53	1.7	0.73	1233	1.09	>5.00	0.65	1254	1.17	>5.00
C5	200 × 120 × 4.5	C30	36	1.7	1.13	1580	1.18	>5.00	1.00	1635	1.31	>5.00
C6	200 × 120 × 6	C30	27	1.7	1.56	2020	1.31	>5.00	1.38	2086	1.46	>5.00
C7	300 × 150 × 4.5	C30	50	2.0	0.83	2383	1.07	>5.00	0.73	2413	1.15	>5.00
C8	300 × 150 × 6	C30	38	2.0	1.14	2891	1.15	>5.00	1.00	2937	1.25	>5.00
C9	300 × 150 × 8	C30	28	2.0	1.57	3491	1.21	>5.00	1.38	3669	1.37	>5.00
C10	300 × 180 × 4.5	C30	53	1.7	0.73	2755	1.08	>5.00	0.65	2823	1.17	>5.00
C11	300 × 180 × 6	C30	40	1.7	1.00	3377	1.18	>5.00	0.88	3503	1.30	>5.00
C12	300 × 180 × 8	C30	30	1.7	1.37	4222	1.30	>5.00	1.21	4410	1.45	>5.00
C13	300 × 300 × 4.5	C30	67	1.0	0.54	4325	1.12	>5.00	0.48	4463	1.21	>5.00
C14	300 × 300 × 6	C30	50	1.0	0.73	5109	1.21	>5.00	0.64	5241	1.30	>5.00
C15	300 × 300 × 8	C30	38	1.0	1.00	6284	1.32	>5.00	0.88	6781	1.52	>5.00
C16	160 × 100 × 3	C60	43	1.6	0.53	1213	1.09	>5.00	0.47	1221	1.14	>5.00
C17	160 × 100 × 4.5	C60	29	1.6	0.83	1510	1.19	>5.00	0.73	1567	1.31	>5.00
C18	160 × 100 × 6	C60	22	1.6	1.15	1749	1.24	>5.00	1.02	2011	1.52	>5.00
C19	200 × 120 × 3	C60	53	1.7	0.43	1681	1.06	2.19	0.38	1678	1.09	>5.00
C20	200 × 120 × 4.5	C60	36	1.7	0.67	1981	1.12	>5.00	0.59	1988	1.17	>5.00
C21	200 × 120 × 6	C60	27	1.7	0.92	2251	1.15	>5.00	0.81	2443	1.32	>5.00
C22	300 × 150 × 4.5	C60	50	2.0	0.49	3186	1.04	2.31	0.43	3209	1.09	>5.00
C23	300 × 150 × 6	C60	38	2.0	0.67	3577	1.07	2.37	0.59	3600	1.13	>5.00
C24	300 × 150 × 8	C60	28	2.0	0.92	4042	1.10	>5.00	0.81	4256	1.23	>5.00
C25	300 × 180 × 4.5	C60	53	1.7	0.43	3778	1.06	2.77	0.38	3778	1.10	4.87
C26	300 × 180 × 6	C60	40	1.7	0.59	4216	1.09	>5.00	0.52	4233	1.15	>5.00
C27	300 × 180 × 8	C60	30	1.7	0.80	4788	1.13	>5.00	0.71	4937	1.23	>5.00
C28	300 × 300 × 4.5	C60	67	1.0	0.32	6050	1.08	>5.00	0.28	6094	1.12	3.93
C29	300 × 300 × 6	C60	50	1.0	0.43	6713	1.13	>5.00	0.38	6800	1.18	>5.00
C30	300 × 300 × 8	C60	38	1.0	0.58	7577	1.18	>5.00	0.52	7767	1.26	>5.00
C31	160 × 100 × 3	C100	43	1.6	0.39	1473	1.07	1.85	0.34	1476	1.11	2.08
C32	160 × 100 × 4.5	C100	29	1.6	0.61	1695	1.12	1.72	0.54	1703	1.18	2.18
C33	160 × 100 × 6	C100	22	1.6	0.85	1938	1.18	>5.00	0.75	2090	1.34	>5.00
C34	200 × 120 × 3	C100	53	1.7	0.32	2088	1.05	1.84	0.28	2077	1.07	1.98
C35	200 × 120 × 4.5	C100	36	1.7	0.49	2359	1.09	1.65	0.43	2350	1.13	1.87
C36	200 × 120 × 6	C100	27	1.7	0.67	2607	1.12	1.60	0.59	2632	1.19	>5.00
C37	300 × 150 × 4.5	C100	50	2.0	0.36	3931	1.03	1.77	0.32	3927	1.06	1.82
C38	300 × 150 × 6	C100	38	2.0	0.49	4278	1.05	1.68	0.43	4282	1.10	1.82
C39	300 × 150 × 8	C100	28	2.0	0.68	4713	1.08	1.55	0.60	4762	1.14	1.86
C40	300 × 180 × 4.5	C100	53	1.7	0.32	4670	1.04	2.14	0.28	4653	1.07	2.30
C41	300 × 180 × 6	C100	40	1.7	0.43	5437	1.15	1.83	0.38	5067	1.11	2.21
C42	300 × 180 × 8	C100	30	1.7	0.59	5617	1.11	1.78	0.52	5629	1.16	2.27
C43	300 × 300 × 4.5	C100	67	1.0	0.23	7549	1.06	>5.00	0.21	7553	1.08	4.44
C44	300 × 300 × 6	C100	50	1.0	0.32	8151	1.09	>5.00	0.28	8149	1.12	4.09
C45	300 × 300 × 8	C100	38	1.0	0.43	8976	1.14	>5.00	0.38	8995	1.18	3.71

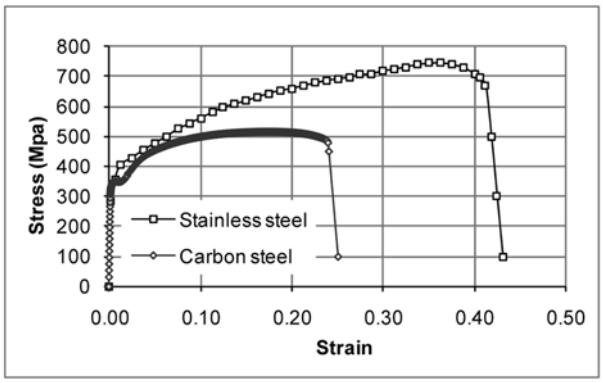

Fig. 9 Typical stress-strain relationships for steel materials

comparing to the equivalent composite columns with carbon steel hollow sections. Fig. 11 compares the maximum loads and corresponding end-shortening of all selected stub concrete-filled columns with stainless steel hollow sections and carbon steel hollow sections. It can concluded that the columns with stainless steel hollow sections provided higher maximum loads if normal or medium strength concrete is used, however for columns filled with high strength concrete the merits using stainless steel hollow sections were less evident. The end-shortening corresponding to the maximum load of the stub column was also compared here. In most cases, the end-shortening of composite columns for both stainless steel and carbon steel section were very close due to the yield strengths of both materials were identical. However also in many cases, especially for composite columns infilling with lower and medium strength concrete, the end-shortening of composite columns formed with stainless steel tubes were

Table 5 Unconfined cylinder strength of infill concrete used in the parametric study

Infill concrete grade reference	Unconfined cylinder strength, f_{ck} (MPa)
C30	37.6
C60	64.0
C100	87.2

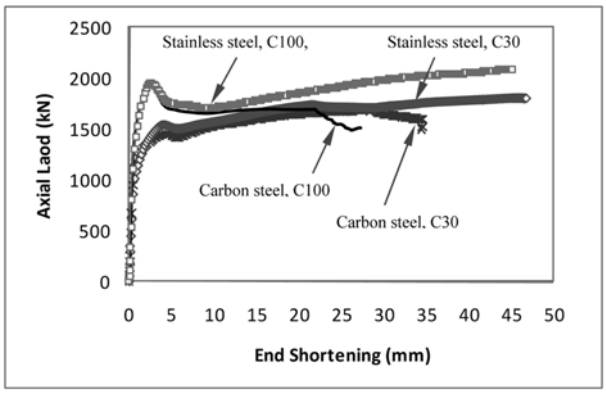

Fig. 10 Comparison of load to end-shortening of concrete-filled stub columns with stainless steel and carbon steel elliptical hollow sections (section 160 × 100 × 6 mm with different concrete grades)

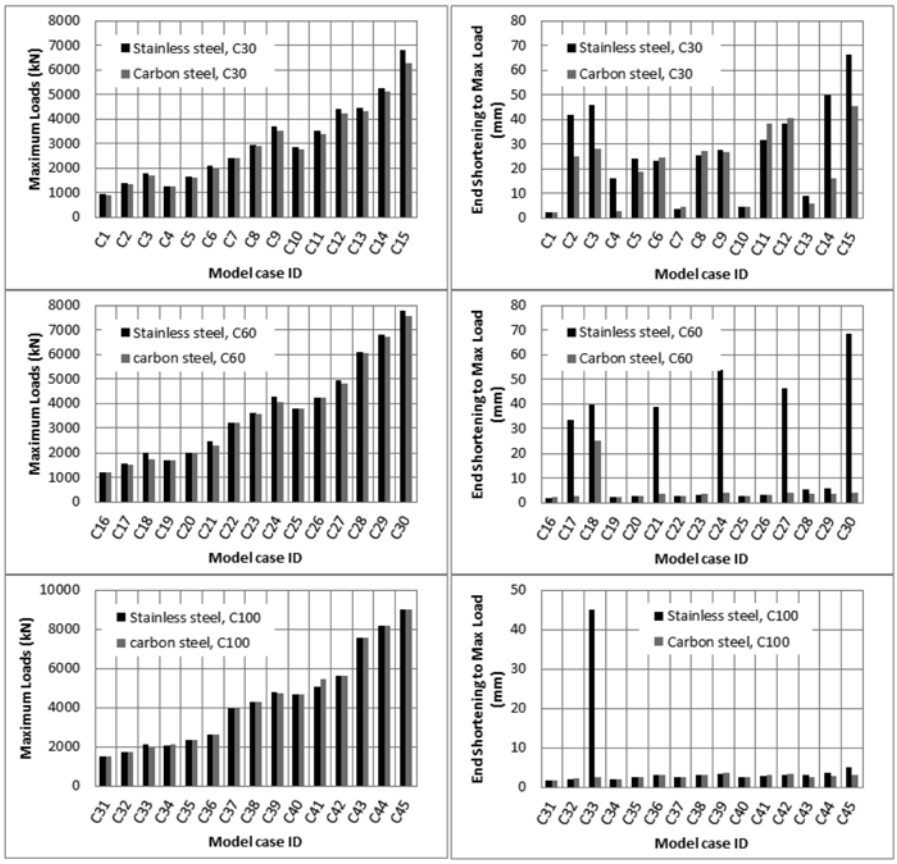

Fig. 11 Comparisons of maximum loads, end-shortening of composite columns using stainless steel and carbon steel hollow sections

evidently higher than that of composite columns formed with carbon steel tube. This resulted from that the ultimate strength and ductility of the stainless steel material were higher than those of carbon steel material, which gave the composite columns formed with stainless steel tubes have a second peak load or better ductility although local yielding might have occurred. Fig. 12 presents a group of typical load vs. end-shortening curves of stub concrete-filled columns with elliptical stainless steel hollow sections. The strength enhancement index, *SI* of 90 selected composite columns in three groups according to the infilled concrete strength is shown in Fig. 13. It can be seen that the range of all strength enhancement indices is between 1.0 to 1.7, which indicates no matter which material of steel is used; stainless steel or carbon steel; the strength of the composite column was higher than the sum of the individual constituent member strengths. This hints that concrete confinement is presented due to the composite action of elliptical concrete-filled steel tubular columns. Furthermore the composite columns with stainless steel hollow sections achieved higher strength-enhancement indices than the equivalent composite columns with carbon steel hollow sections.

Fig. 14 shows the effect of section constraining factor, ξ to the strength enhancement index, *SI*. It can be seen, regardless of the concrete strength and the steel material properties, the strength enhancement index increases with the increases in the section constraining factor. This indicates that the increases in

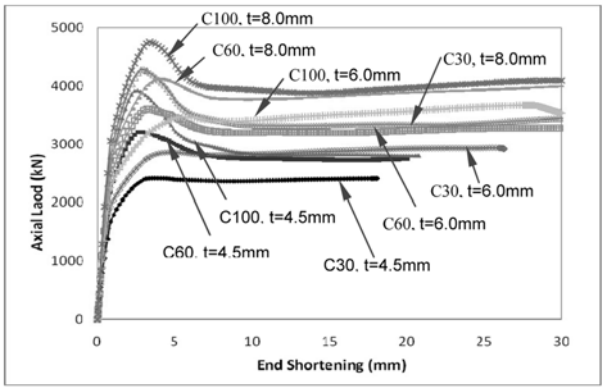

Fig. 12 Comparison of load to end-shortening curves of typical concrete-filled stub columns with elliptical stainless steel hollow sections (section 300 × 150 × t with different concrete grades)

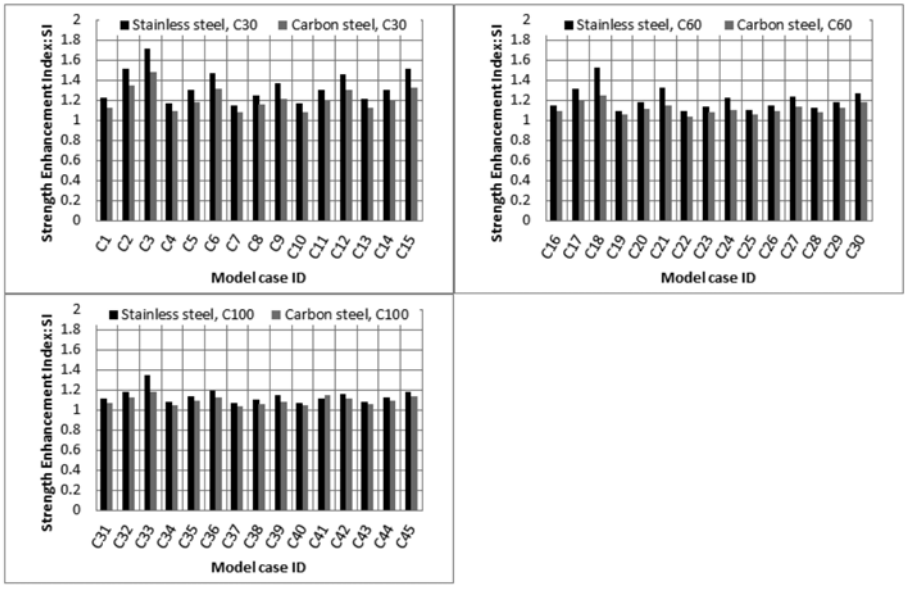

Fig. 13 Comparison of strength enhancement indices of concrete-filled composite columns with stainless steel and carbon steel hollow sections

steel hollow section confinement improved the composite action in a concrete-filled steel tubular column. Furthermore, it would appear that the average strength enhancement index for composite columns filled with lower strength concrete is higher than that of columns filled with higher strength concrete, this suggested that there is efficiency to be made for using low strength concrete in concrete-filled columns.

Fig. 15 presents the effect of section strength factor γ to the strength enhancement index, *SI*. It would appear that with the increases in the section strength factor, the strength enhancement index reduced. This indicates that the composite action of concrete-filled column reduces with the decreases in wall thickness of hollow section or increases in the section diameter. For concrete-filled columns with identical section dimensions, the strength enhancement index of columns filled with lower strength

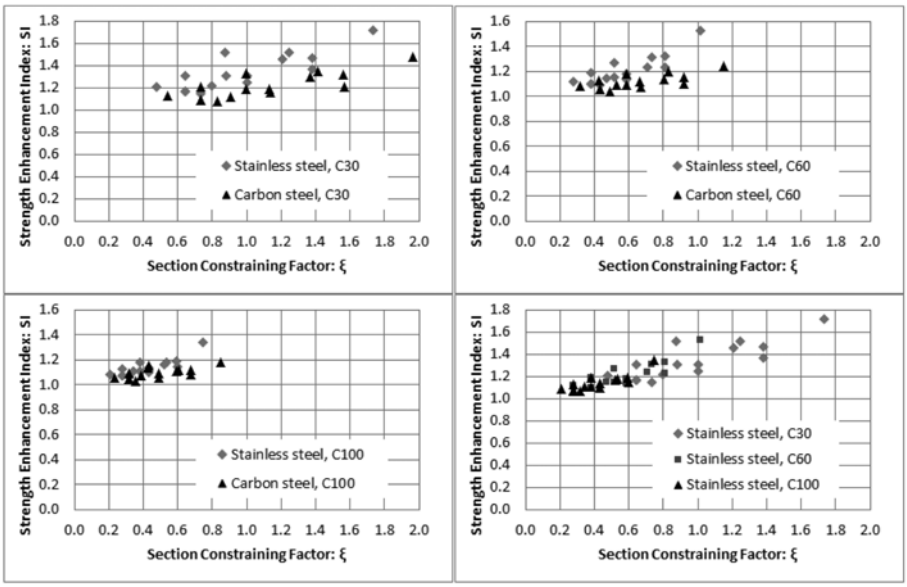

Fig. 14 Effect of section constraining factor to strength enhancement index

concrete was evidently higher than that of columns filled with higher strength concrete.

Fig. 16 compares the effect of the section aspect ratio α to the strength enhancement index *SI* of composite columns with different section wall thickness and concrete strength. It shows that: (1) with the increases in the section aspect ratio, the strength enhancement index decreases. This observation is more evident for columns with thicker section wall thickness; (2) for concrete-filled columns with

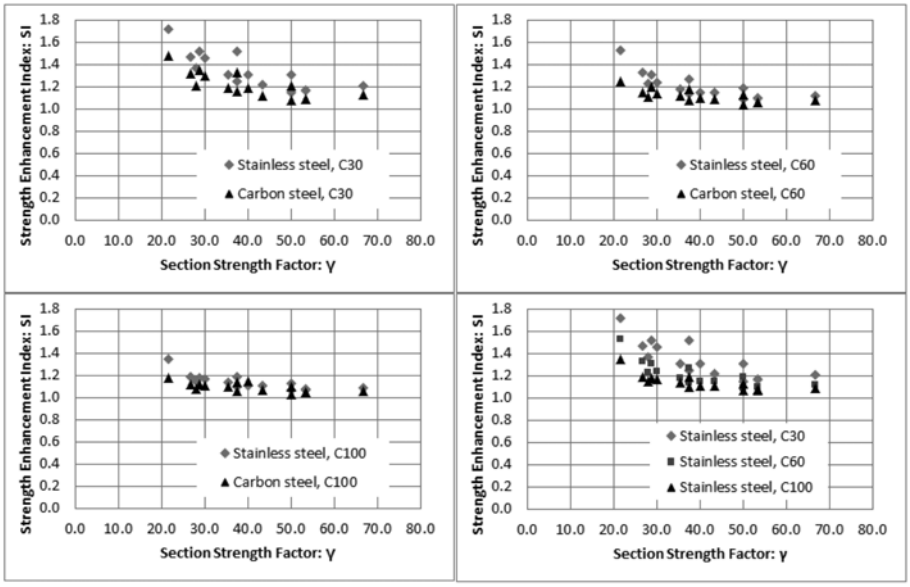

Fig. 15 Effect of section strength factor to strength enhancement index

identical section aspect ratio, the strength enhancement index increases when the concrete strength reduces or the section wall thickness increases; (3) columns with circular hollow section ($\alpha = 1$) provides the higher strength enhancement index than the columns with elliptical hollow sections ($\alpha > 1$).

From Fig. 17, it can be seen that all the ductility indices were greater than 1.5. Figs. 18 and 19 compared the effects of section constraining factor, ξ and section strength factor, γ to the ductility index, *DI.* All the composite columns filled with normal strength concrete (C30) shows excellent ductility and all having value of the ductility index greater than 5. In these figures, all ductility indices greater than 5 were set as 5 for convenience. For the composite columns filled with medium (C60) and high strength (C100) concrete, the ductility index of the columns with stainless steel hollow section were higher than those with carbon steel hollow sections. However for some stub columns with circular hollow sections filled with higher strength concrete, such as cases C28, C43, C44 and C45, the composite columns with carbon steel hollow section achieved higher ductility index.

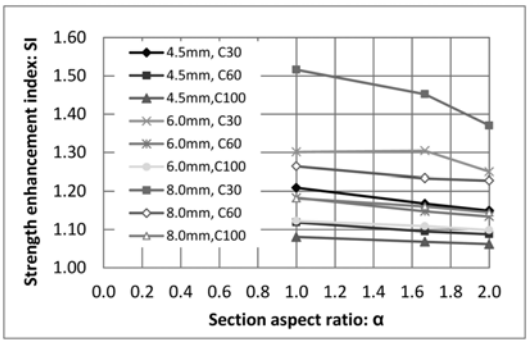

Fig. 16 Effect of section aspect ratio to strength enhancement index

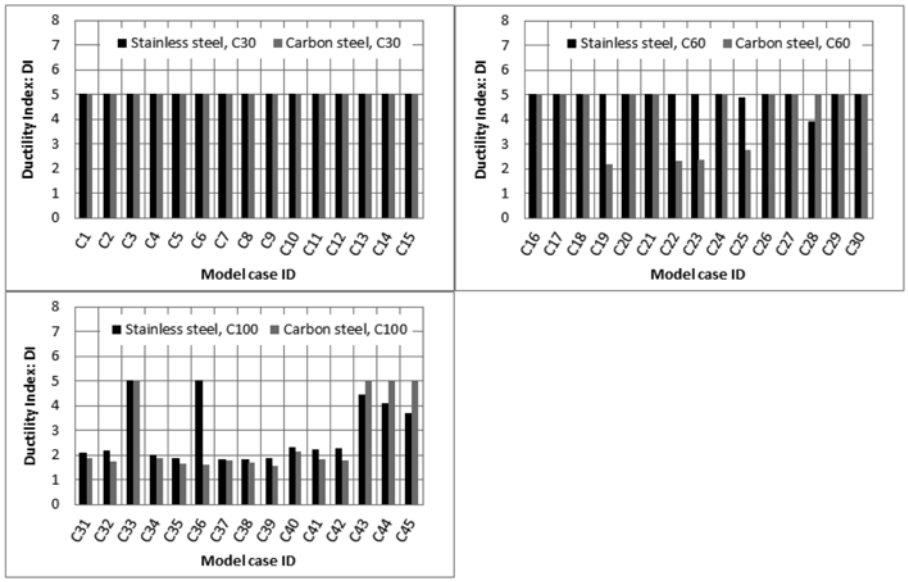

Fig. 17 Comparison of ductility index of concrete-filled columns with stainless steel and carbon steel hollow sections

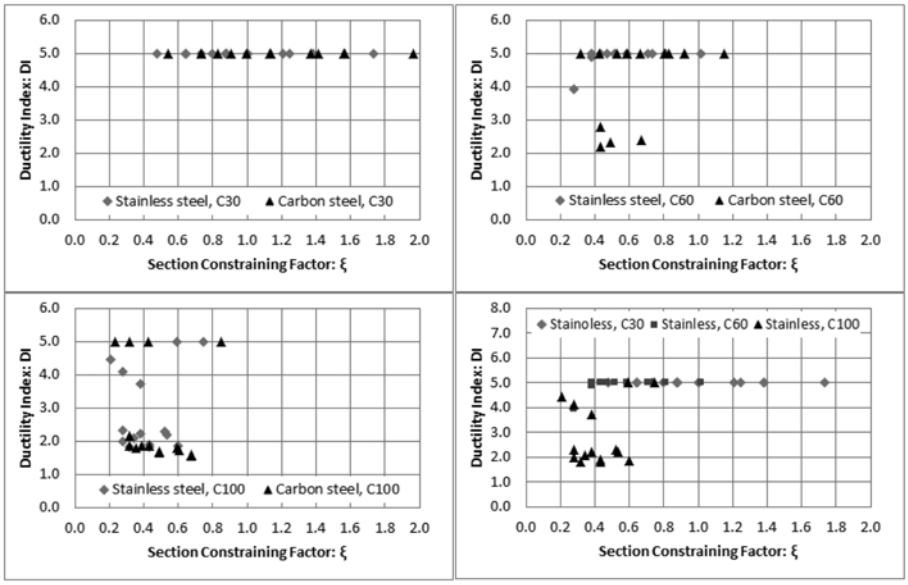

Fig. 18 Effect of section constraining factor to column ductility index

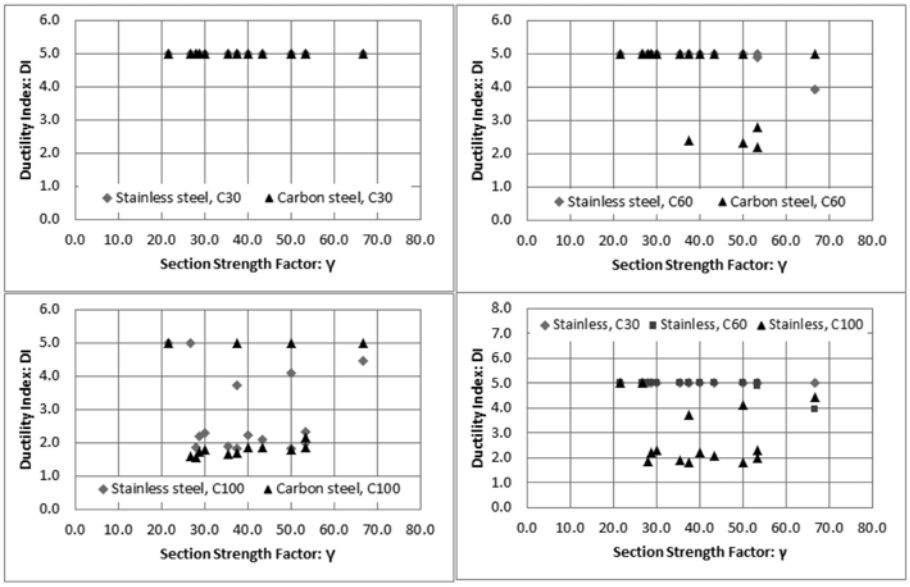

Fig. 19 Effect of section strength factor to column ductility index

6. Conclusions

A finite element method is developed using ABAQUS/Standard solver with the proposed confined concrete stress-strain model and is verified via experimental studies. Parametric study for concrete-filled stub composite columns, covering various sectional features: $\gamma = (a + b)/t = 22\sim67$; $\alpha = a/b = 1\sim2$;

concrete grades, C30~C100 and two steel material properties: high strength stainless steel and carbon steel (S355), were conducted to investigate the effects of section geometry and material properties to the axial compressive behaviour. Based on the research results presented in this paper, the following conclusions can be made

1. The nonlinear finite element method developed through ABAQUS/Standard solver, combining with the proposed compressive stress-strain model for confined concrete in elliptical (including circular) hollow sections, may be used to predict the axial compressive behaviour of stub elliptical concrete-filled steel tubular columns.
2. Concrete-filled stub columns with both elliptical stainless steel and carbon steel hollow sections provided satisfactory strength enhancement index *SI* (1.0~1.7) and ductility index *DI* (greater than 1.5) in the range of the selected columns in this research. Furthermore the strength enhancement index and ductility index of stub columns with stainless steel hollow sections were higher than those of identical composite columns with carbon steel hollow sections and this suggests the advantages of using stainless steel in concrete-filled tubular columns. This observation is especially evident for columns filled with normal (C30) strength concrete.
3. The section constraining factor, ξ, section strength factor, γ and section aspect ratio, α, shown that the section geometric features and material properties of the composite columns affect the structural behaviour of stub elliptical concrete-filled steel tube columns. Based on the research results presented in this paper, the following points may been drawn: (1) columns with higher section constraining factor, ξ achieved higher strength enhancement index, *SI* and ductility index, *DI*; (2) the strength enhancement index, *SI* and ductility index, *DI* decreases with the increases of the section strength factor, γ; (3) the strength enhancement index, *SI* decreases with the section aspect ratio, α increases, but the change of the ductility index, *DI* was not evident; (4) the strength enhancement index *SI* and ductility index *DI* reduced with the promotion of concrete grades.
4. In the finite element modelling, the confined concrete compressive stress-stain model significantly affected the compressive behaviour of stub composite columns. The confined concrete compressive stress-stain model proposed in this paper introduced many assumptions in particular after concrete cracked. Although some empirical data from other literatures were referred to, further experimental investigation is necessary to confirm the confined compressive stress-stain model of concrete with elliptical composite columns.

Acknowledgements

The research reported in this paper is funded by the research grant from the Engineering and Physical Science Research Council (EP/G002126/1) in the UK who are gratefully acknowledged.

References

ACI 318-95(1999), *Building code requirements for structural concrete and commentary*, Detroit (USA), American Concrete Institute.

Chan T.M. and Gardner L. (2008a), "Bending strength of hot-rolled elliptical hollow sections", *J. Constr. Steel Res.*, **64**(9), 971-986.

Chan T.M. and Gardner L. (2008b), "Compressive resistance of hot-rolled elliptical hollow section", *Eng. Struct.,*

30(2), 522-532.
Chan T.M. and Gardner L. (2009), "Flexural Buckling of Elliptical Hollow Section Columns", *J. Struct. Eng-ASCE* , **135**(5), 546-557.
CEN(2006), BS EN 1993-1-4: 2006, Eurocode 3: *Design of steel structures: Part 1-4: General rules-Supplementary rules for stainless steels*, Committee of European Normalisation, British Standards Institution, London.
Dabaon, M., El-Khoriby S., El-Boghdadi, M. and Hassanein, M. F. (2009),"Confinement effect of stiffened and unstiffened concrete-filled stainless steel tubular stub columns", *J. Const. Steel, Res.*, **65**(8-9), 1846-1854.
Dai, X. and Lam, D. (2010), "Numerical modelling of the axial compressive behaviour of short concrete-filled elliptical steel columns", *J. Constr. Steel Res.*, **66**(7), 931-942.
Ellobody, E. and Young, B. (2005), "Structural performance of cold-formed high strength stainless steel columns", *J. Constr. Steel Res.*, **61**(12), 1631-1649.
Ellobody, E. and Young, B. (2006), "Design and behaviour of concrete-filled cold-formed stainless steel tube columns", *Eng. Struct.*, **28**(5), 716-728.
Ellobody, E., Young, B. and Lam, D. (2006), "Behaviour of normal and high strength concrete-filled compact steel tube circular stub columns", *J. Constr. Steel Res.,* **62**(7), 706-715.
EN 10002-1 (2001), Metallic materials - Tensile testing - Part 1: Method of test at ambient temperature, British Standard Institute, UK.
Gardner L. and Chan T.M. (2007), "Cross-section classification of elliptical hollow sections", *Steel. Compos. Struct.*, **7**(3), 185-200.
Gardner, L., Cruise, R.B., Sok, C.P., Krishnan, K. and Ministro dos Santos J. (2007), "Life cycle costing of metallic structures", *Proceedings of the Institution of Civil Engineers-Engineering Sustainability*, **160**(4), 166-177.
Gardner, L., Talja, A. and Baddoo, N.R. (2006), "Structural design of high strength austenitic stainless steel", *Thin. Wall. Struct.*, **44**(5), 517-528.
Giakoumelis, G. and Lam, D. (2004), "Axial capacity of circular concrete filled tube columns", *J. Constr. Steel Res.*, **60**(7), 1049-1068.
Gibbons, C. and Scott, D. (1996), "Composite hollow steel tubular columns filled with high strength concrete", *Proceedings international conference on advances in steel structures*, 467-476.
Han, L.H. (2002), "Tests on stub columns of concrete-filled RHS sections", *J. Constr. Steel Res.*, **58**(3), 353-372.
Han, L.H. and Yang, Y. (2001), "Influence of concrete compaction on the behaviour of concrete filled steel tubes with rectangular sections", *Adv. Struct. Eng.*, **4**(2), 93-108.
Han, L.H. and Yao, G.H. (2003), "Influence of concrete compaction on the strength of concrete filled steel RHS columns", *J. Const. Steel Res.,* **59**(6), 751-767.
Han, L.H. and Yao, G.H. (2004), "Experimental behaviour of thin walled hollow structural steel (HSS) columns filled with self consolidating concrete (SCC)", *Thin. Wall. Struct.*, **42**(9), 1357-1377.
Hu, H.T. and Schnobrich, W.C. (1989), "Constitutive modelling of concrete by using non-associated plasticity", *J. Mater. Civil. Eng.*, **1**(4), 199-216.
Hu, H.T., Huang, C.S., Wu, M.H. and Wu, Y.M. (2003), "Nonlinear analysis of axially loaded concrete-filled tube columns with confinement effect", *J. Struct. Eng-ASCE*, **129**(10), 1322-1329.
Lam, D. and Gardner, L. (2008), "Structural design of stainless steel concrete filled columns", *J. Constr. Steel Res.*, **64**(11), 1275-1282.
Lam, D. and Williams, C.A. (2004), "Experimental study on concrete filled square hollow sections", *Steel. Compos. Struct.*, **4**(2), 95-112.
Mursi, M. and Uy, B. (2003), "Strength of concrete filled steel box columns incorporating interaction buckling", *J. Struct. Eng-ASCE*, **129**(5), 626-639.
O'Shea, M.D. and Bridge, R.Q. (1997), "The design for local buckling of concrete filled steel tubes", *Composite Constructive-Conventional and Inovate*, Innsbruck, Austria, 319-324.
O'Shea, M.D. and Bridge, R.Q. (2000), "Design of circular thin-walled concrete filled steel tubes", *J. Struct. Eng-ASCE*, **126**(11), 1295-1303.
Rangan, B.V. and Joyce, M. (1992), "Strength of eccentrically loaded lender steel tubular columns filled with high strength concrete", *ACI Struct. J.*, **89**(6), 676-681.

Richart, F.E. and Brandzaeg, A. and Brown, R.L. (1928), "A study of the failure of concrete under combined compressive stresses", *Bull. 185. Champaign (IL, USA)*, University of Illinois Engineering Experimental Station.
Ruiz-Teran A.M. and Gardner L. (2008), "Elastic buckling of elliptical tubes", *Thin. Wall. Struct.*, **46**(11), 1304-1318.
Saenz, L.P. (1964), "Discussion of 'Equation for the stress-strain curve of concrete' by P. Desayi, and S. Krishnan", *ACI J.*, **61**(9), 1229-1235.
Sakino, K., Tomii, M. and Watanabe, K. (1998), "Sustaining load capacity of plain concrete stub columns by circular steel tubes", *Conference on concrete filled steel tubular construction*, 112-118.
Schneider, S.P. (1998), "Axially loaded concrete-filled steel tubes", *J. Struct. Eng-ASCE,* **124**(10), 1125-1138.
Theofanous M. Chan T.M. and Gardner L. (2009a), "Flexural behaviour of stainless steel oval hollow sections", *Thin. Wall. Struct.*, **47**(6-7), 776-787.
Theofanous M., Chan T.M. and Gardner L. (2009b), "Structural response of stainless steel oval hollow section compression members", *Eng. Struct.*, **31**(4), 922-934.
Uy, B. (1998a), "Concrete filled fabricated steel box columns for multi-storey buildings", *Prog. Struct. Eng. Mater.*, **1**(2), 150-158.
Uy, B. (1998b), "Local and post-local buckling of concrete filled steel welded box columns", *J. Constr. Steel Res.*, **47**(1-2), 47-72.
Uy, B. (2001a), "Static long-term effects in short concrete-filled steel box columns under sustained loading", *ACI Struct. J.*, **98**(1), 96-104.
Uy, B. (2001b), "Strength of short concrete filled high strength steel box columns", *J. Constr. Steel Res.*, **57**(2), 113-134.
Yang, H., Lam, D. and Gardner, L. (2008), "Testing and analysis of concrete-filled elliptical hollow sections", *Eng. Struct.*, **30**(12), 3771-3781.
Young, B. and Ellobody, E. (2006), "Experimental investigation of concrete-filled cold-formed high strength stainless steel tube columns", *J. Constr. Steel. Res.*, **62**(5), 484-492.
Young, B. and Lui, W.M. (2005), "Behaviour of cold-formed high strength stainless steel sections", *J. Struct. Eng-ASCE*, **131**(11), 1738-1745.

CC